

Electronic Supplementary Information (ESI)

Iron(III)-bipyridine incorporated metal-organic frameworks for photocatalytic reduction of CO₂ with improved performance

Yuan-Ping Wei,^{‡,a} Sizhuo Yang,^{‡,b} Peng Wang,^a Jin-Han Guo,^a Jier Huang^{*,b} and Wei-Yin Sun^{*,a}

^a Coordination Chemistry Institute, State Key Laboratory of Coordination Chemistry, School of Chemistry and Chemical Engineering, Nanjing National Laboratory of Microstructures, Collaborative Innovation Center of Advanced Microstructures, Nanjing University, Nanjing 210023, China

^b Department of Chemistry, Marquette University, Milwaukee, Wisconsin 53201, United States

*Corresponding Authors: jier.huang@marquette.edu; sunwy@nju.edu.cn

SECTION 1. Ligand synthesis

SECTION 2. UiO synthesis

SECTION 3. Steady state X-ray absorption spectroscopy (XAS)

SECTION 4. Gas adsorption experiments

SECTION 5. UV-Vis diffuse reflectance spectra

SECTION 6. Electrochemical characterization

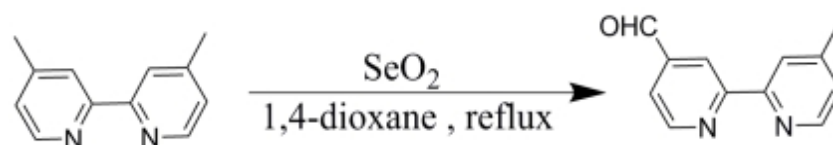
SECTION 7. Photochemical CO₂ conversion experiments

SECTION 8. References

SECTION 1. Ligand synthesis

Materials and methods. Ligand amino-triphenyldicarboxylic acid (amino-TPDC) was prepared as reported previously.¹ 4,4'-Dimethyl-2,2'-bipyridine were purchased from Energy Chemical. SeO₂ was obtained from Alfa Chemical, other chemicals and solvents are of reagent grade obtained from Sinopharm Chemical Reagent Co., Ltd without further purification. ¹H-NMR spectra were measured on Bruker-DRX 400 MHz instruments at room temperature.

Synthesis of 4'-methyl-[2,2'-bipyridine]-4-carbaldehyde.



In accordance with a modified procedure reported previously,² a mixture of 4,4'-dimethyl-2,2'-bipyridine (1.00 g, 5.4 mmol), SeO₂ (660 mg, 5.9 mmol) and 1,4-dioxane (50 mL) was added to a round-bottom flask, which was heated to reflux for 2 days. After a time, the yellow suspension became a black precipitate. The reaction was hot filtered quickly. After cooled to room temperature, the solution was filtered again. The resulting residue was collected through a rotary evaporator from the yellow filtrate, then was dissolved in ethyl acetate and filtered again. The filtrate was extracted with 1.0 M NaOH and 0.3 M Na₂S₂O₅ successively, then the aqueous phase was extracted with CHCl₃ again. The organic phase was evaporated to yield pure 4'-methyl-[2,2'-bipyridine]-4-carbaldehyde (37%). IR (KBr pellet cm⁻¹) 3050 (m), 3023 (m), 1720 (s), 1620 (s), 1530 (m), 1285 (s), 1145 (m), 675 (m). ¹H NMR (400 MHz, CDCl₃): δ = 2.50 (s, 3H), 7.21 (d, 1H), 7.74 (dd, 1H), 8.31 (s, 1H), 8.61 (d, 1H), 8.86 (s, 1H), 8.93 (d, 1H), 10.21 (s, 1H).

SECTION 2. UiO synthesis

Materials and methods. UiO-68-NH₂ was prepared as reported previously,¹ other chemicals and solvents are of reagent grade obtained from Sinopharm Chemical Reagent Co., Ltd and used without further purification. Powder X-ray diffraction (PXRD) data were collected on a Bruker D8 Advance X-ray diffractometer with Cu-K α ($\lambda = 1.5418 \text{ \AA}$) radiation. Scanning electron microscopy (SEM) measurements were performed on a Hitachi S-4800 field emission scanning electron microscope at an accelerating voltage of 5 kV. Thermogravimetric analyses (TGA) were performed by means of TGA-DSC1 thermal analyzer (Mettler-Toledo Instrumentation) in the temperature range of 30-800 °C under a nitrogen atmosphere with a heating rate of 10 °C min⁻¹. Fourier transform Infrared (FT-IR) spectra were recorded using KBr discs in the range of 400-4000 cm⁻¹ on a Bruker Vector 22 FT-IR spectrophotometer. X-ray photoelectron spectroscopy (XPS) was performed on UIVAC-PHI 5000 VersaProbe using monochromatized Al K α at $h\nu = 1486.6 \text{ eV}$. The C 1s peak was used as the reference peak. ¹H-NMR spectra were measured on Bruker-DRX 400 MHz instruments at room temperature.

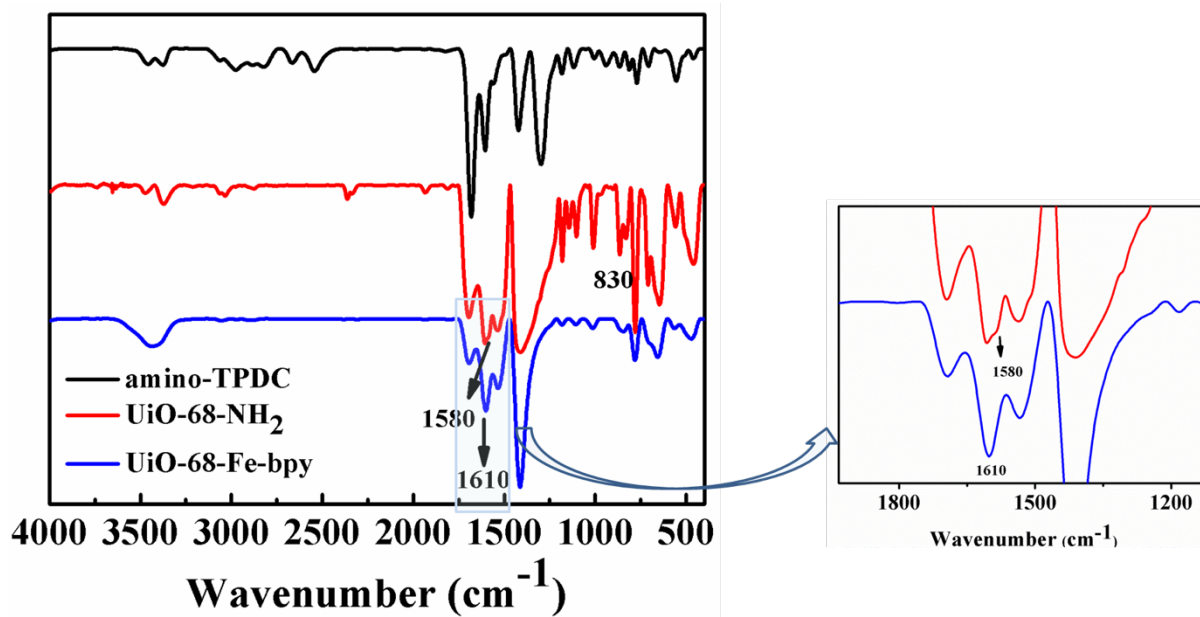


Fig. S1 IR spectra of amino-TPDC, UiO-68-NH₂ and UiO-68-Fe-bpy.

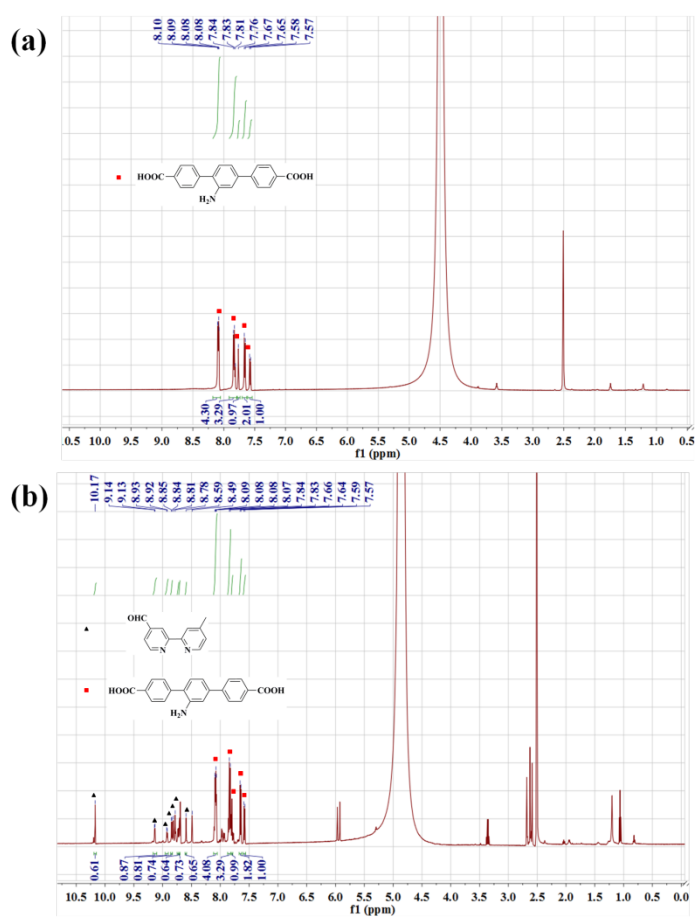


Fig. S2 ¹H NMR spectra of the digested (a) UiO-68-NH₂ and (b) UiO-68-bpy in HF/DMSO-*d*₆.

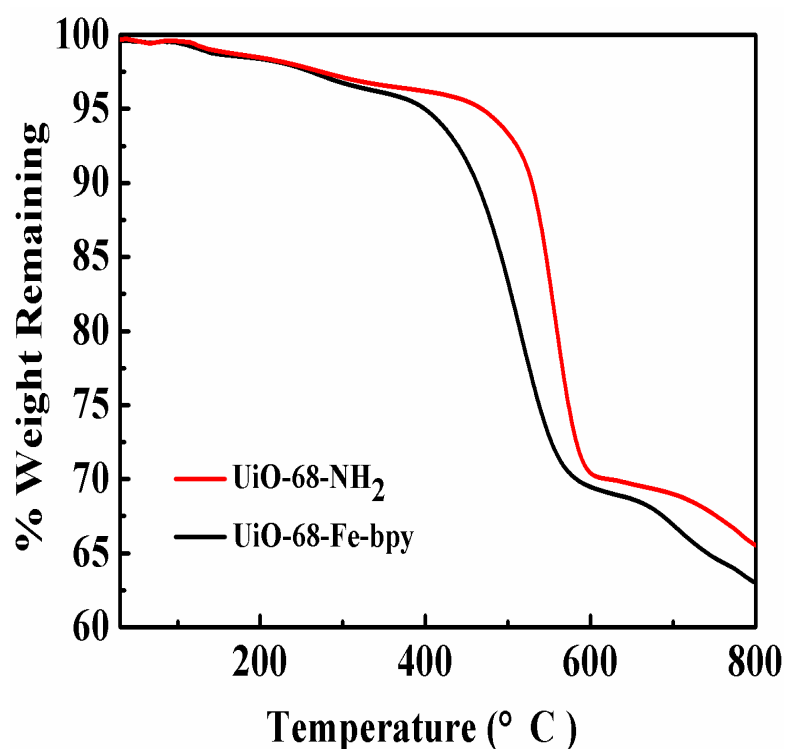


Fig. S3 TG traces of UiO-68-NH₂ and UiO-68-Fe-bpy.

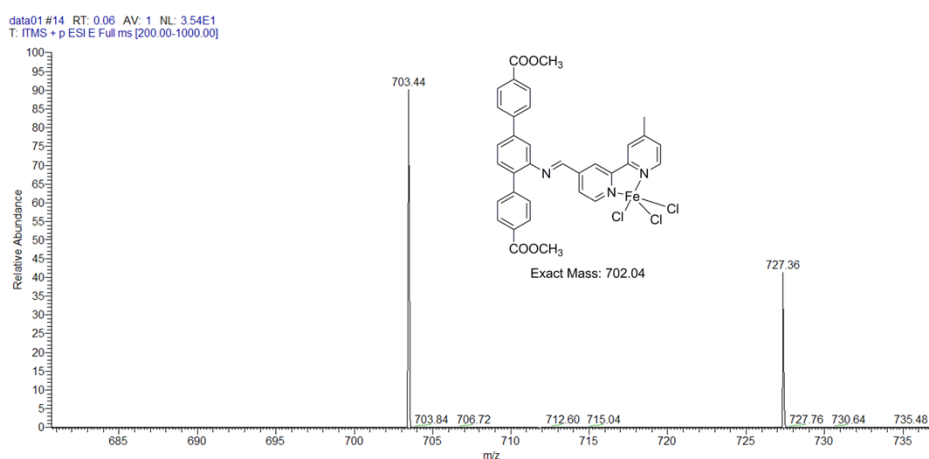


Fig. S4 MS spectrum of TPDC-Fe-bpy (TPDC-Fe-bpy was synthesized by the esterified amino-TPDC, 4'-methyl-[2,2'-bipyridine]-4-carbaldehyde, FeCl₃ using the method of UiO-68-Fe-bpy) (The weak coordinated DMF molecule is lost under acidic condition).

SECTION 3. Steady state X-ray absorption spectroscopy (XAS)

XAS measurements were performed at the beamline 12BM-B at the Advanced Photon Source of Argonne National Laboratory. The Extend X-ray Absorption Fine Structure spectra (EXAFS) were collected at room temperature by fluorescence mode using a 13-element germanium solid-state detector. One ion chamber is placed before the sample and used as the incident X-ray flux reference signal. Samples were scanned at the Fe edge. Fe foil was scanned at the same time for energy calibration.

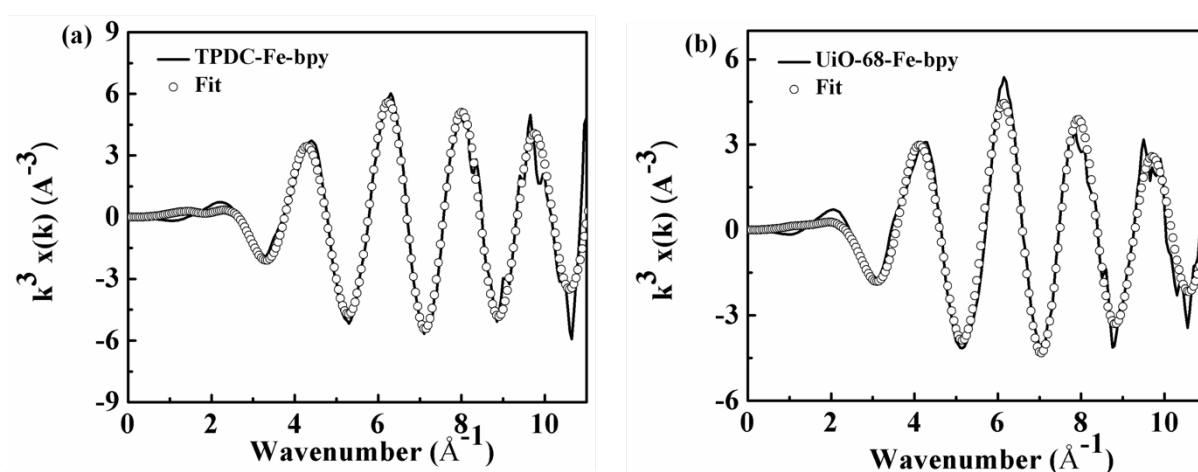


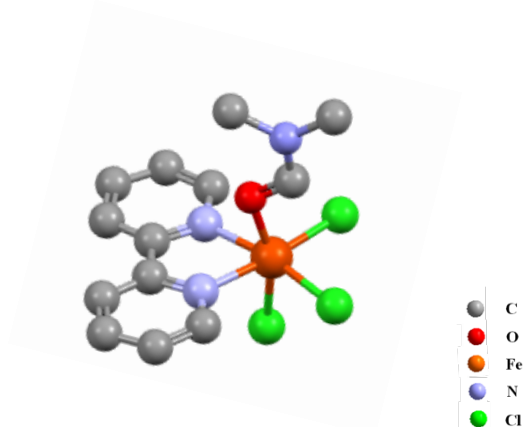
Fig. S5 The X-ray absorption spectra in k-space of (a) TPDC-Fe-bpy and (b) UiO-68-Fe-bpy at Fe K-edge. The solid lines and open circles are experimental and fitted results, respectively.

Table S1. Summary of EXAFS fitting parameters for TPDC-Fe-bpy.

	$\Delta E0$ (ev)	CN	R (\AA)	$\sigma^2 \times 10^{-3}$ (\AA^2)
Fe-N	-5.357	2	2.11	2
Fe-Cl		3	2.18	6

Table S2. Summary of EXAFS fitting parameters for UiO-68-Fe-bpy.

	$\Delta E0$ (ev)	CN	R (\AA)	$\sigma^2 \times 10^{-3}$ (\AA^2)
Fe-N	-7.569	2	2.07	2
Fe-Cl		3	2.18	10



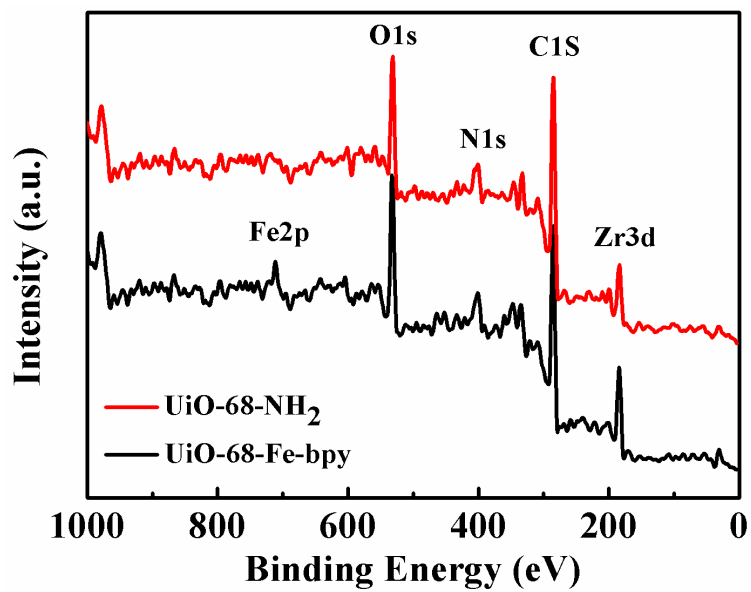


Fig. S6 XPS spectra of UiO-68-NH₂ and UiO-68-Fe-bpy.

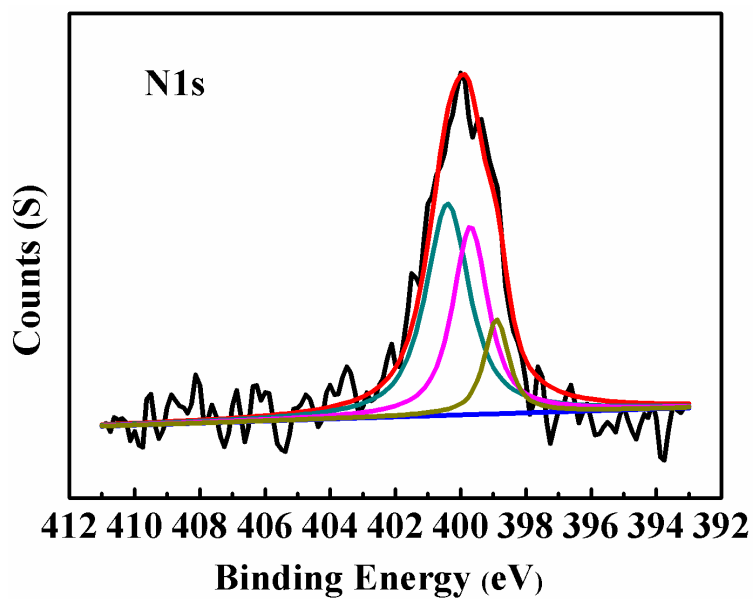


Fig. S7 N 1s spectrum of UiO-68-Fe-bpy.

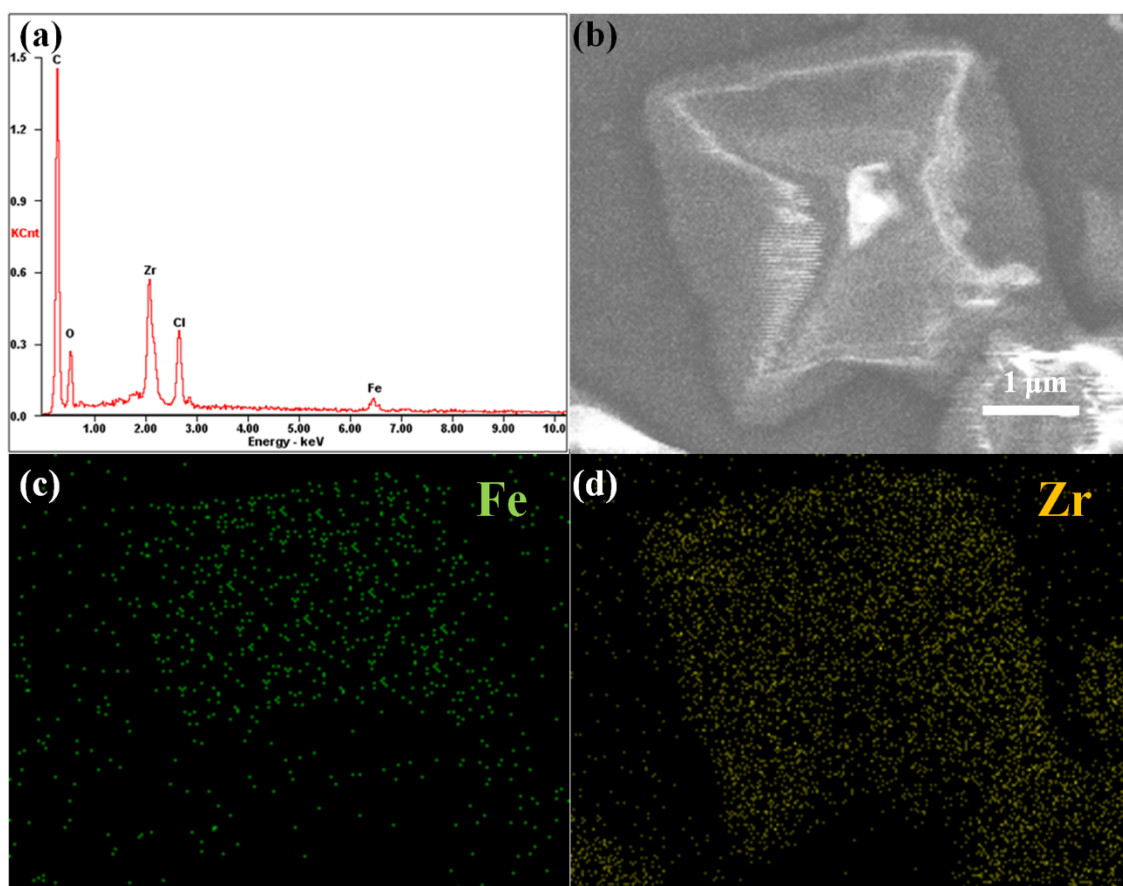


Fig. S8 (a) EDS spectrum and (b) SEM image of UiO-68-Fe-bpy. SEM-mapping images of (c) Fe and (d) Zr in UiO-68-Fe-bpy.

SECTION 4. Gas adsorption experiments

Materials and methods. N₂ and CO₂ used in adsorption experiments were 99.999% grade obtained from Tianhong Gas. Prior to gas adsorption experiments, the samples were soaked in acetone to exchange DMF, followed by evacuation under a dynamic vacuum at 120 °C for 10 h. The TG traces (Fig. S14, ESI†) and PXRD patterns (Fig. S15, ESI†) indicated that the structures of UiO-68-NH₂ and UiO-68-Fe-bpy were well maintained after the removal of solvent. All the gas adsorption isotherms were measured on a Belsorp-max volumetric gas sorption analyzer by employing a standard volumetric technique up to saturated pressure. The N₂ adsorption isotherms were monitored at 77 K, while CO₂ adsorption isotherms were obtained at 273 and 298 K.

1) N₂ adsorption isotherms

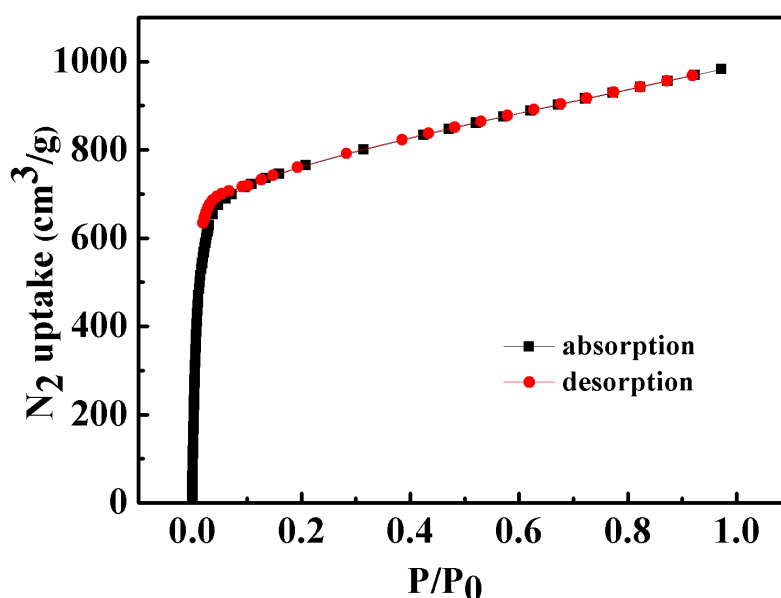


Fig. S9. Nitrogen adsorption isotherms (at 77 K) of UiO-68-NH₂. UiO-68-NH₂ has the BET surface area of 2589.7 m²/g.

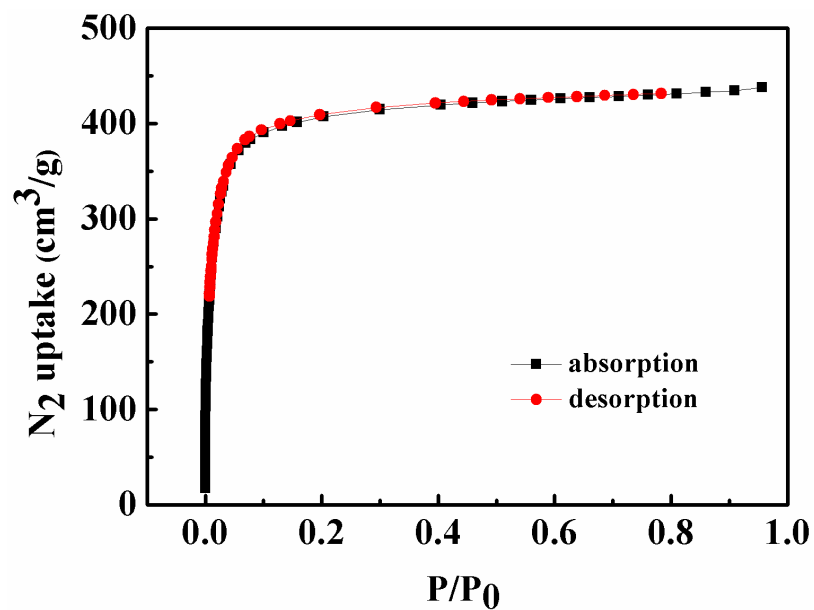


Fig. S10 Nitrogen adsorption isotherms (at 77 K) of UiO-68-Fe-bpy. UiO-68-Fe-bpy has the BET surface area of 1372.1 m²/g.

2) CO₂ adsorption isotherms

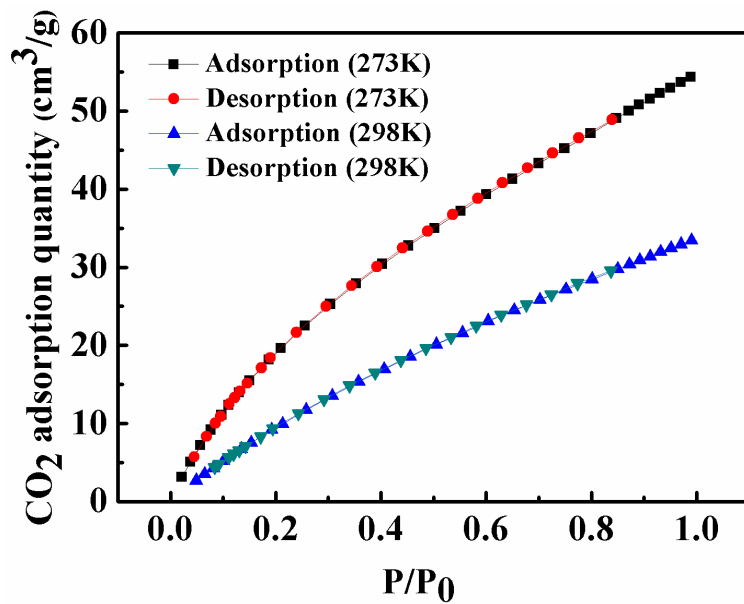


Fig. S11 CO₂ adsorption and desorption isotherms for UiO-68-NH₂ at 273 and 298 K.

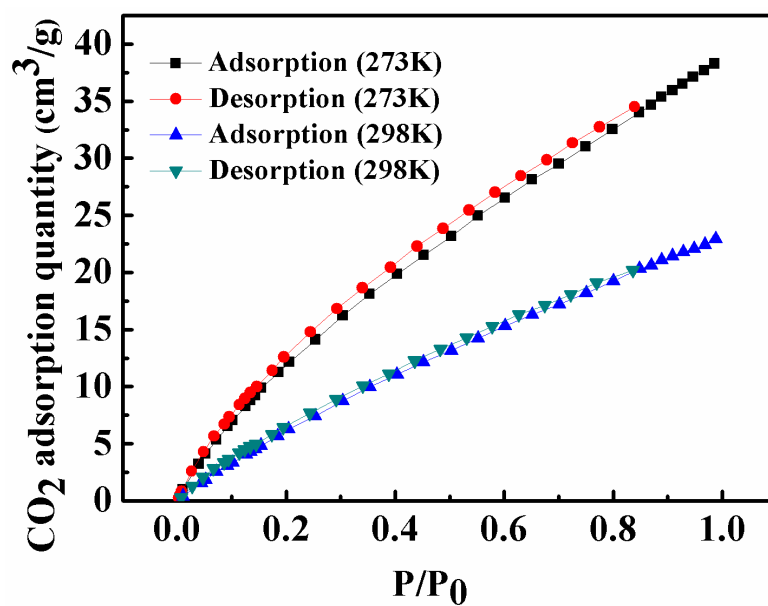


Fig. S12 CO₂ adsorption and desorption isotherms for UiO-68-Fe-bpy at 273 and 298 K.

3) Pore size distribution

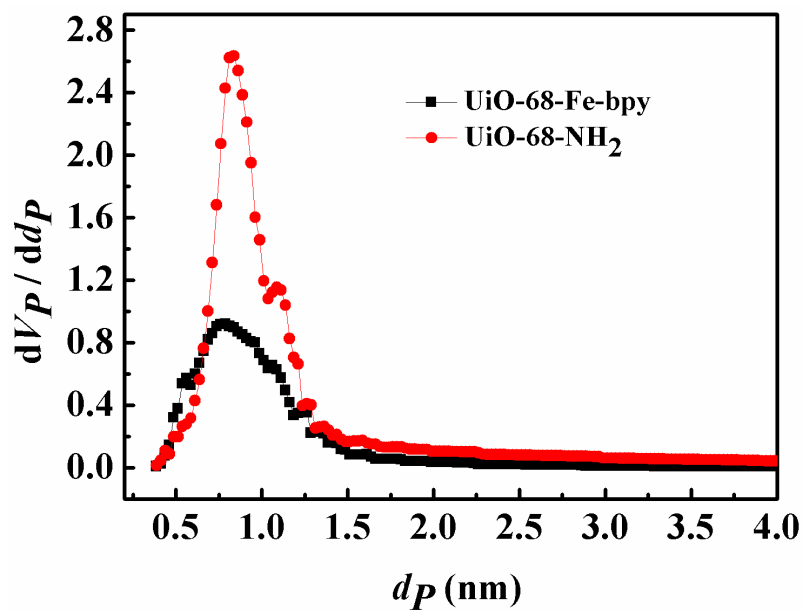


Fig. S13 Pore size distribution for UiO-68-NH₂ and UiO-68-Fe-bpy evaluated by using N₂ adsorption data measured at 77 K.

SECTION 5. UV-Vis diffuse reflectance spectrum

Materials and methods. BaSO₄ for UV-Vis diffuse reflectance spectrum was purchased from Sigma-Aldrich. UV-Vis diffuse reflectance data were recorded on a Shimadzu UV-3600 spectrophotometer in the wavelength range of 200-1200 nm, a white standard of BaSO₄ was used as reference.

Evaluate the band gaps of MOFs by UV-Vis diffuse reflectance spectrum. As most of the literatures have mentioned, MOFs can act as semiconductor during the photochemical CO₂ conversion process, we tried to determine the band gap (E_g) of the MOFs by UV-Vis diffuse reflectance spectra. Tauc plot was employed to determine the E_g of the materials, we adopted

$$(\alpha h\nu)^2 = A(h\nu - E_g)$$

to evaluate the band gap.

Notations:

α	absorption coefficient, dimensionless
h	Planck constant, $h = 4.136 \times 10^{-15}$ eV s
ν	frequency, s ⁻¹
A	constant, eV ^{-1/2}
E_g	band gap, eV

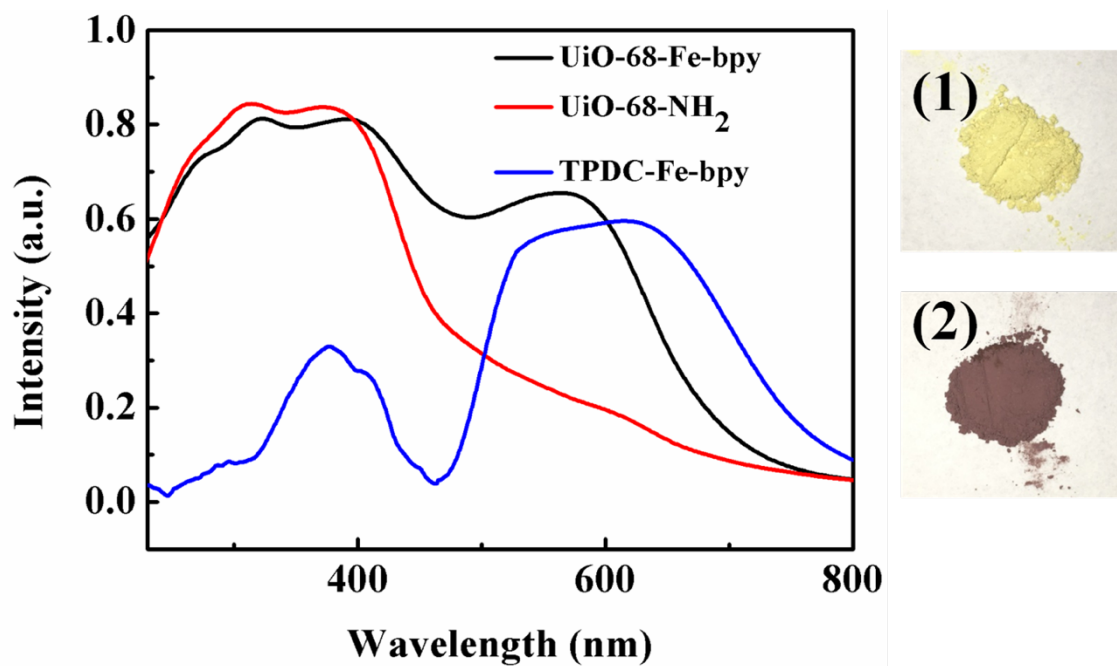


Fig. S14 UV-vis spectra of UiO-68-NH₂, TPDC-Fe-bpy and UiO-68-Fe-bpy (right: photograph of (1) UiO-68-NH₂ and (2) UiO-68-Fe-bpy).

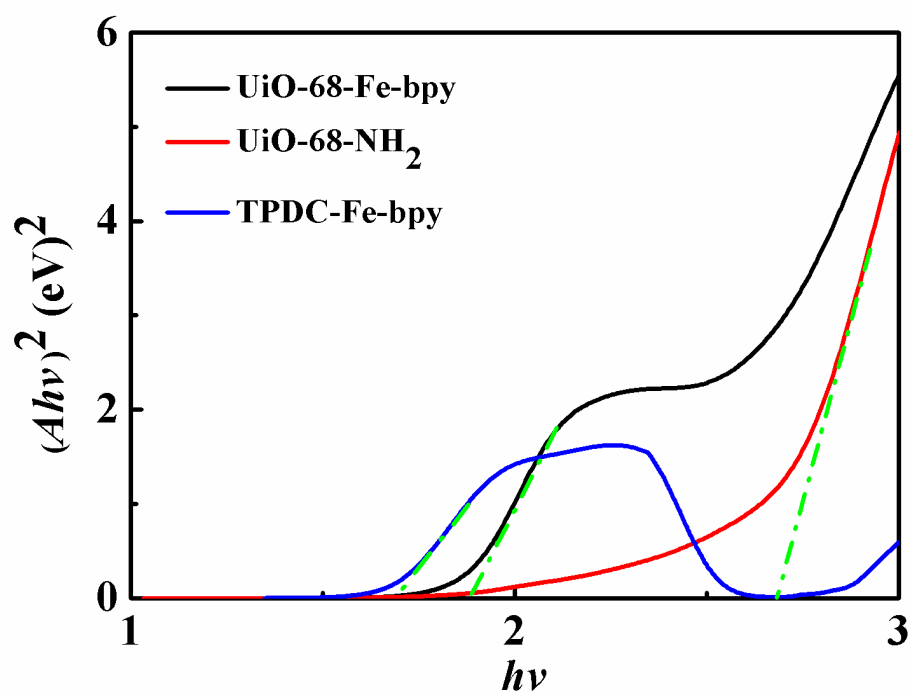


Fig. S15 Tauc plots of UiO-68-NH₂, TPDC-Fe-bpy and UiO-68-Fe-bpy.

SECTION 6. Electrochemical characterization

Materials and methods. MeOH (99.9%, Extra Dry, with molecular sieves, water \leq 30 ppm (by K.F.)), Na₂SO₄ was purchased from Energy Chemical. ultrapure water (18 M Ω) used in the experiments was supplied by a Millipore System (Millipore Q), argon (99.999%) was obtained from Tianhong gas, other chemicals and solvents are of reagent grade obtained from Sinopharm Chemical Reagent Co., Ltd without further purification. The as-synthesized sample (2 mg) was dispersed into 1 mL MeOH, and then 10 μ L Nafion was added.

Cyclic voltammetry. Cyclic voltammetry was performed on a CHI 730E electrochemical work station (Chenhua Instrument, Shanghai, China) in a standard three-electrode system with DMF + 0.1 M *n*-Bu₄NPF₆ used as the electrolyte at 0.1 V s⁻¹. The working electrode was glassy carbon electrode (3mm-diameter, Gaoss Union, Wuhan). The counter-electrode was a platinum wire and the reference electrode was an aqueous SCE electrode.

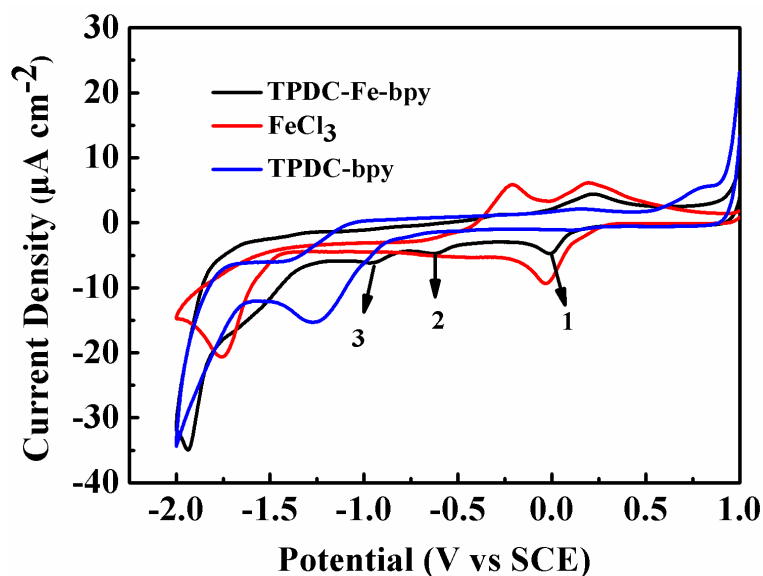


Fig. S16 Cyclic voltammograms of TPDC-Fe-bpy (black), TPDC-bpy (blue) and FeCl_3 (red) in CO_2 saturated solutions. (TPDC-Fe-bpy was synthesized by the esterified amino-TPDC, 4'-methyl-[2,2'-bipyridine]-4-carbaldehyde, FeCl_3 using the method of UiO-68-Fe-bpy).

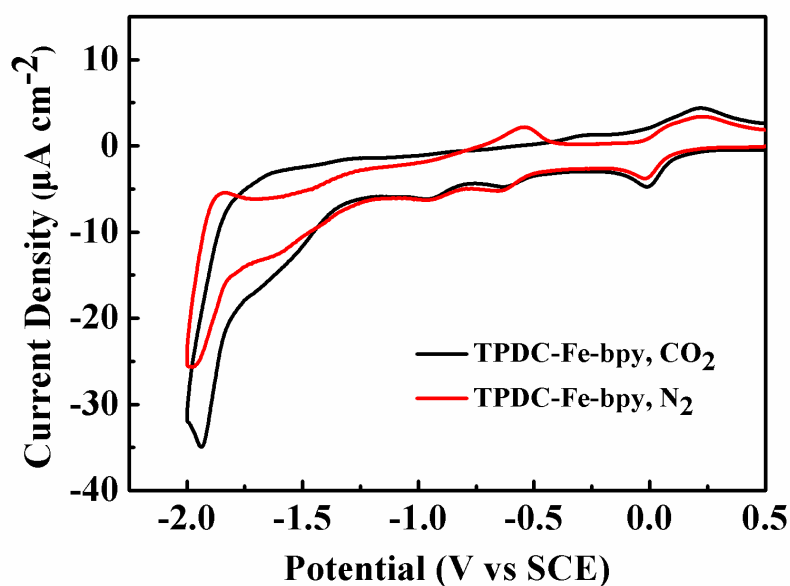


Fig. S17 Cyclic voltammograms of TPDC-Fe-bpy in CO_2 (black) and N_2 (red) saturated solutions.

SECTION 7. Photochemical CO₂ conversion experiments

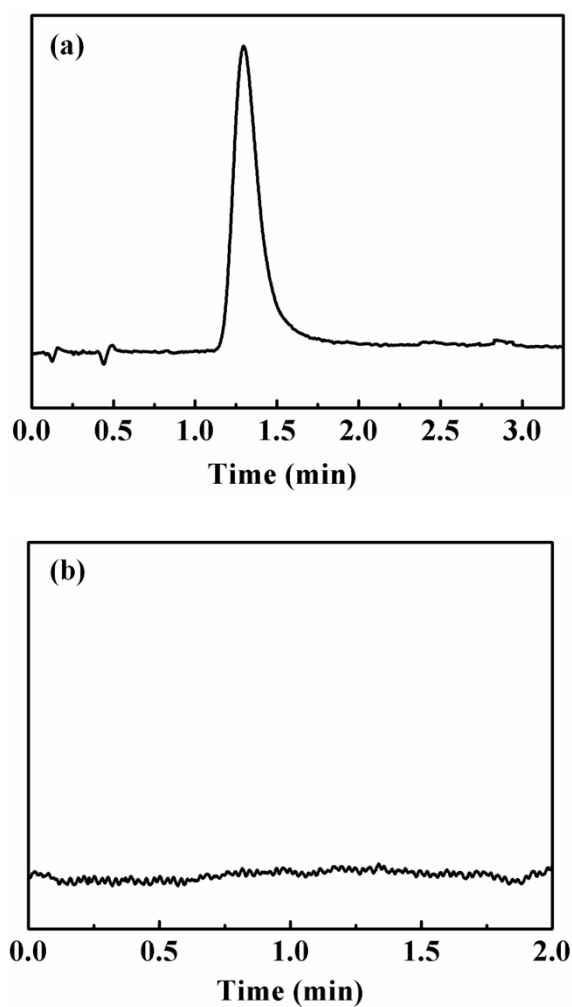


Fig. S18 Typical gas chromatogram observed during long-term irradiation: (a) FID detector for CO and CH₄ monitoring, CO was detected with retention time of about 1.290 min, however, no CH₄ (retention time: 2.540 min) was detected; (b) TCD detector for H₂ detecting, which showed no H₂ (retention time: 0.578 min) was detected.

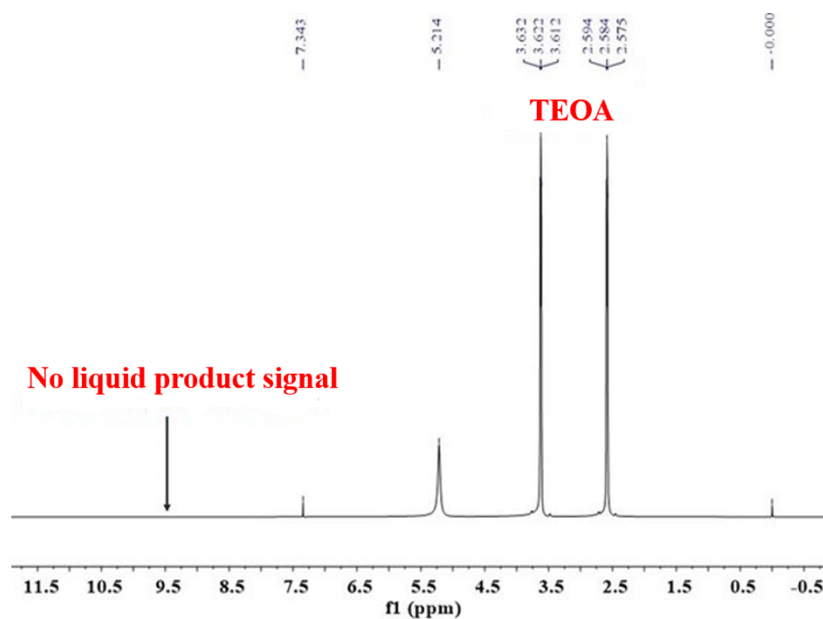


Fig. S19 $^1\text{H-NMR}$ spectrum used to detect the liquid product from the photocatalytic reaction.

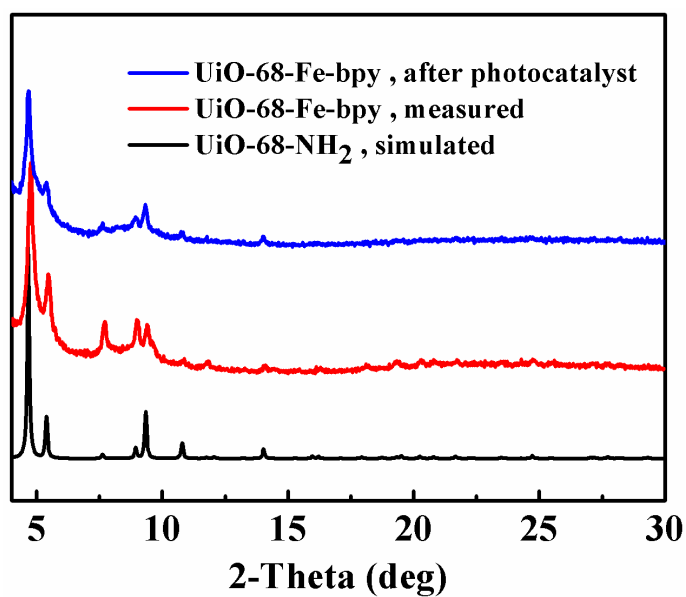


Fig. S20 XRPD patterns of simulated UiO-68-NH₂, UiO-68-Fe-bpy before and after 18 h photocatalysis.

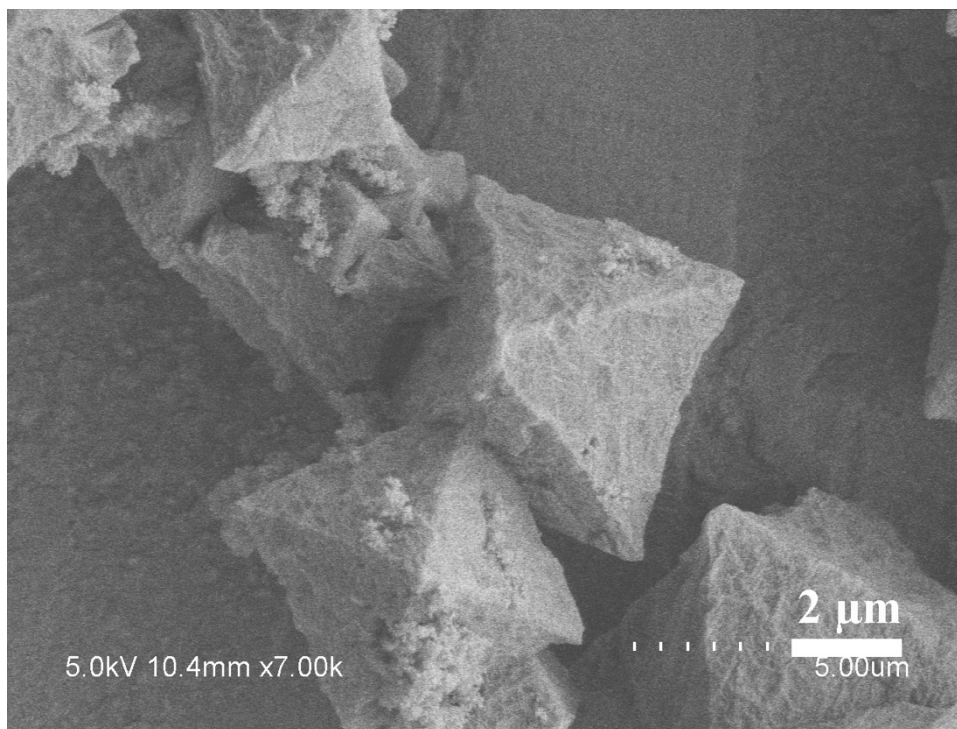


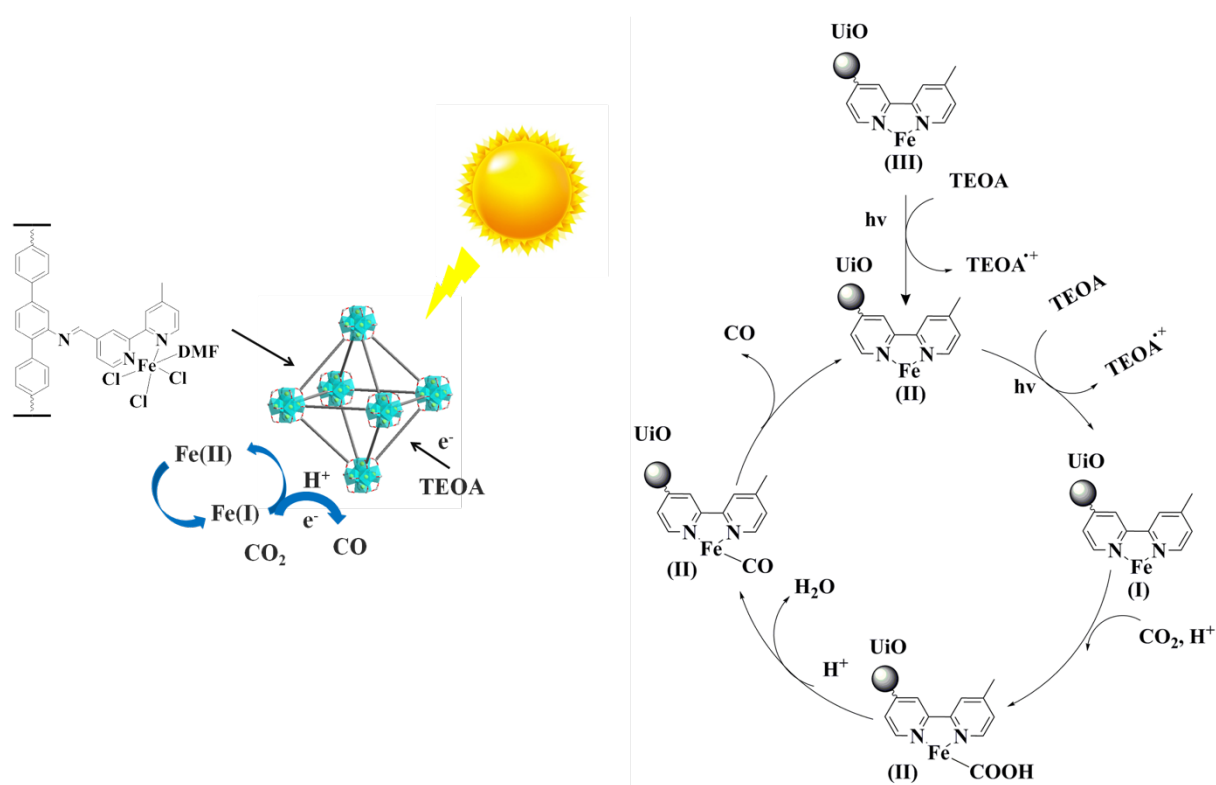
Fig. S21 SEM image of UiO-68-Fe-bpy after 18 h photocatalysis.

Table S3. Summary of photocatalytic CO₂ reduction performances over various visible light response photocatalysts

Photocatalyst	Products	CO Evolution for 6 h (μmol)	Light source Xe lamp (W)	Ref.
UiO-68-Fe-bpy	CO	10	300	This work
UiO-68-NH ₂	CO	106	300	This work
TPDC-Fe-bpy	CO	21	300	This work
NH ₂ -MIL-53(Fe)	CO	15	300	3
NH ₂ -MIL-88B(Fe)	CO	50	300	3
CdS/TiO ₂	CO	50	300	4

Table S4. ICP measurement for UiO-68-Fe-bpy after every run of photocatalysis

run (reaction for 6 h)	Fe content [wt%]	Selection [%]	CO Evolution [$\mu\text{mol/g}$]
1	0.58	100	106
2	0.57	100	103
3	0.51	100	105



Scheme S1. Proposed mechanism for photocatalytic CO₂ reduction over the as-prepared UiO-68-Fe-bpy under visible light.

SECTION 8. References

- (1) Y. Wei, Y. Liu, F. Guo, X. Dao, W. Sun, *Dalton Trans.* 2019, **48**, 8221-8226.
- (2) M. Brain, T. Glennt, E. Stephen, J. Gerald, J. Thomas, *Int. J. Pept. Protein Res.* 1991, **38**, 114-123.
- (3) X. Y. Dao, J. H. Guo, Y. P. Wei, F. Guo, Y. Liu, W. Y. Sun, *Inorg. Chem.* 2019, **58**, 8517–8524.
- (4) X. Pan, Y. Xu, *J. Phys. Chem. C* 2015, **119**, 7184-7194.